Journal of Computational Physics 227 (2008) 8909–8921

Contents lists available at ScienceDirect

Journal of Computational Physics

journal homepage: www.elsevier.com/locate/jcp

Pseudo-wave decomposition high-order method for magnetogasdynamics

T. Gomez*

d'Alembert Institute, Université Pierre et Marie Curie, Paris 6, Case 162, 4 Place Jussieu, 75252 Paris Cedex 05, France

ARTICLE INFO

Article history:
Received 18 January 2007
Received in revised form 30 June 2008
Accepted 3 July 2008
Available online 15 July 2008

PACS:
47.35.−i
47.35.Tv
44.05.+e

Keywords:
Magnetohydrodynamics
Riemann invariant
Characteristics method
DRP schemes

ABSTRACT

A new characteristics-based decomposition of the ideal magnetogasdynamic equations is derived. This formulation consists in representing the temporal variation of the physical quantities pressure, velocity, magnetic field and entropy as a linear combination of the generic advective terms corresponding to each wave type occurring in the medium. The flux terms can then be handled with existing high-order upwind dispersion relation preserving schemes; those being specifically chosen in our case to increase numerical accuracy and improve stability. Another feature of the new formulation of the non-ideal governing equations is that the boundary conditions are *exactly* satisfied at the frontiers of the computational domain. The accuracy of the method is assessed by comparison between numerical and exact solutions. Good agreement is obtained between computed and exact solutions.

1. Introduction

Recent research has shown that compressible flows may be modified significantly by magnetic Lorentz forces provided by the interaction between the conducting medium and a magnetic field [14–17]. Therefore, flow control by magnetic field action could be an efficient process to reduce drag due to turbulence in aerospace applications by suppressing or enhancing the boundary layer instability and transition. Another challenge is the control of the magneto-aeroacoustic noise, which could be realized by using electromagnetic/fluid interactions in the boundary layer and/or by using optimal transpiration boundary control as done for the aeroacoustic flows [1]. The physical understanding of these approaches requires to consider fluid dynamics, electromagnetics, molecular physics and chemical kinetics, among others. In this paper, we will consider the first two of these, within the hypothesis of non-ideal magnetohydrodynamics (MHD). The MHD equations result from merging the Maxwell and Navier–Stokes equations in the so-called non-ideal MHD form. This MHD formulation is obtained under the hypothesis of negligible displacement current density, negligible density charge and finite electrical conductivity of the gas.

The development of new algorithms to solve the equations of compressible continuum MHD deals essentially with upwind or characteristics-based schemes issued from the proper eigensystem of ideal MHD equations. Examples of these methods solving Riemann problem in the direction normal to a cell face, can be found in [2,11]. Characteristics-based methods have already been implemented into two-dimensional codes for both ideal and non-ideal cases [10,6]. A more recent approach consists in using high-order spatially implicit schemes (Padé-type) [5,8] in conjunction with high-order filters for non-ideal three-dimensional MHD [3]. The high-order filters are needed to avoid the small scale instabilities generated by

* Tel.: +33 014 427 5466.
E-mail address: gomez@lmm.jussieu.fr

0021-9991/$ - see front matter © 2008 Elsevier Inc. All rights reserved.
doi:10.1016/j.jcp.2008.07.001

the finite difference schemes without deterioration of the accuracy. This very versatile approach can be used in multidisciplinary applications to solve the equations governing the dynamics of the flow.

In the present paper, the eigenstructure of the ideal MHD equations is examined with the idea of deriving high resolution computational algorithms for turbulent flows as well as for acoustic problem. Starting from the MHD model equations, a pressure-velocity-magnetic field-entropy formulation of the MHD equations is given in a non-conservative form. Such numerical methods have already been successfully exploited in the case of compressible Navier–Stokes equations [7,13,9,1]. For instance, upwind methods are very efficient and highly appreciated for aerospace applications in the high speed regime. They require a well founded knowledge of wave propagation phenomena which should be strongly incorporated in this numerical method. Indeed in the MHD case, this formulation takes into account the contribution of each wave-type wc/Slow magnetoacoustic, Alfvén and entropy waves to the temporal variations of the physical quantities. Therefore, high-order upwind dispersion relation preserving is used for each wave-type flux term appearing in the equations providing high stability and accuracy properties to the method. Moreover, this formulation allows to specify exact wall boundary conditions as shown in Section 5. Two examples of inflow condition implementations are given in Section 5, showing how the boundary conditions can be exactly imposed for both the non-reflecting and the subsonic flow cases. In addition, four validation cases are simulated with a two-dimensional code to analyse the method accuracy and validate the code. Conclusions are given in Section 8.

2. Governing equations

The governing equations of MHD are obtained by coupling the pre-Maxwell equations to the Navier–Stokes equations. The coupling consists in adding the Lorentz force to the momentum equation and electromagnetic energy terms to the energy equation. The pre-Maxwell equations are derived from the complete Maxwell equations and are written as follows using SI units:

$$\nabla \times \mathbf{H} = \mathbf{j} + \frac{\partial \mathbf{D}}{\partial t}, \tag{1}$$

$$\nabla \times \mathbf{E} = -\frac{\partial \mathbf{B}}{\partial t}, \tag{2}$$

$$\nabla \cdot \mathbf{B} = 0, \tag{3}$$

$$\nabla \cdot \mathbf{D} = q, \tag{4}$$

where $\mathbf{E}$ and $\mathbf{H}$ are the electric and magnetic field vectors, $\mathbf{D} = \epsilon_0 \mathbf{E}$ is the electric displacement, $\mathbf{j}$ is the current density vector, $\mathbf{B}$ is the magnetic induction vector, and q is the charge density. The two important assumptions of MHD are (i) $\epsilon\omega/\sigma \ll 1$ and (ii) $(\|\mathbf{u}\|/c)^2 \ll 1$, where ϵ is the dielectric constant, ω the plasma frequency, σ the electrical conductivity, $\mathbf{u}$ the medium velocity, and c the speed of light. The assumption (i) permits to discard the displacement current term $\frac{\partial \mathbf{D}}{\partial t}$ in the Ampère–Maxwell equation (1). The second assumption (ii) allows to ignore the relativistic effects. Indeed, we consider the case where typical flow length scales are much larger than the Debye length, flow time scales are larger than the reciprocal of the plasma frequency, and flow velocities are much less than the speed of light. The constitutive relations are then written as

$$\mathbf{B} = \mu_{\mathrm{m}} \mathbf{H}, \tag{5}$$

$$\mathbf{j} = \boldsymbol{\sigma} \cdot (\mathbf{E} + \mathbf{u} \times \mathbf{B}), \tag{6}$$

where μ_{m} is the magnetic permeability and Eq. (6) is the generalized Ohm's law in which the convection, polarization, Hall, and ion-slip current components have been neglected. The electrical conductivity tensor can be approximated by a scalar value if the collision frequency is much greater than the cyclotron (gyro) frequency, as is the case in a relatively dense gas. The equations are, thus, pertinent in the paradigm of strongly collision dominated plasmas.

The equation describing the magnetic induction evolution may be written as

$$\frac{\partial \mathbf{B}}{\partial t} + \nabla \times \left[\frac{1}{\sigma} \left(\nabla \times \frac{\mathbf{B}}{\mu_{\mathrm{m}}} \right) - \mathbf{u} \times \mathbf{B} \right] = 0 \tag{7}$$

by eliminating the electric field $\mathbf{E}$ in Faraday's law (2) with the help of Ohm's law (6) and substituting $\mathbf{j}$ in Faraday's law from the Ampere–Maxwell law (1). Equivalently, this equation may be written in conservation form as

$$\frac{\partial \mathbf{B}}{\partial t} + \nabla \cdot (\mathbf{u}\mathbf{B} - \mathbf{B}\mathbf{u}) + \nabla \times \left[\frac{1}{\sigma} \left(\nabla \times \frac{\mathbf{B}}{\mu_{\mathrm{m}}} \right) \right] = 0. \tag{8}$$

The equations describing the fluid motion are the Navier–Stokes equations. The continuity equation remains unchanged, whereas the momentum equation contains the extra electromagnetic body force term $F_{\mathrm{em}} = \mathbf{j} \times \mathbf{B}$, which may be written:

$$F_{\mathrm{em}} = \mathbf{j} \times \mathbf{B} = \nabla \cdot (\mathbf{B}\mathbf{B}/\mu_{\mathrm{m}}) - \nabla(\mathbf{B}^2/\mu_{\mathrm{m}}), \tag{9}$$

where $\nabla \cdot \mathbf{B} = 0$ has been employed. The momentum equation may therefore be written as

$$\frac{\partial \rho \mathbf{u}}{\partial t} + \nabla \cdot \left[\rho \mathbf{u}\mathbf{u} + \left(p + \frac{\mathbf{B}\cdot\mathbf{B}}{2\mu_{\mathrm{m}}} \right)\mathbf{I} - \frac{\mathbf{B}\mathbf{B}}{\mu_{\mathrm{m}}} \right] - \nabla \cdot \boldsymbol{\tau} = 0, \tag{10}$$

where p is the static pressure, $\mathbf{B}\cdot\mathbf{B}/\mu_{\mathrm{m}}$ is the magnetic pressure. The shear stress tensor $\boldsymbol{\tau}$ is defined in terms of the molecular viscosity μ by

$$\boldsymbol{\tau} = \mu \left[(\nabla + \nabla^{\mathrm{T}})\mathbf{u} - \frac{2}{3}(\nabla \cdot \mathbf{u})\mathbf{I} \right], \tag{11}$$

where $\mathbf{I}$ denotes the identity tensor and 'T' the transpose.

The energy equation is obtained by adding the electromagnetic energy term E_{m}:

$$E_{\mathrm{m}} = \mathbf{E}\cdot\mathbf{j} = (\mathbf{j}/\sigma - \mathbf{u}\times\mathbf{B})\cdot\mathbf{j} = \frac{1}{\sigma}\left(\nabla \times \frac{\mathbf{B}}{\mu_{\mathrm{m}}} \right)^2 - (\mathbf{u}\times\mathbf{B})\cdot\left(\nabla \times \frac{\mathbf{B}}{\mu_{\mathrm{m}}} \right), \tag{12}$$

where $\mathbf{j}^2/\sigma$ is the Joule heating term and $-\mathbf{u}\times\mathbf{B}\cdot\mathbf{j} = \mathbf{u}\cdot\mathbf{j}\times\mathbf{B}$ is the work done by the Lorentz force. The Joule heating drives internal energy variations and the Lorentz force contributes to kinetic energy variations. The energy conservation equation may be written in conservation law form by introducing the total energy term $Z = e + \frac{1}{2}\mathbf{u}^2 + \mathbf{B}^2/(2\mu\rho)$ where $e = p/(\gamma-1)\rho$ is the internal energy.

It is assumed that the transport coefficients μ, κ, σ are known functions of the state variables T and ρ so it only remains to specify the state equation for T and e. These follow from the assumption that the plasma behaves like a perfect gas.

The non-ideal MHD equations can be written by using $\mathbf{b} \equiv \mathbf{B}/\sqrt{\mu}$ as follows:

$$\frac{\partial \rho}{\partial t} + \nabla \cdot (\rho \mathbf{u}) = 0, \tag{13}$$

$$\frac{\partial \rho \mathbf{u}}{\partial t} + \nabla \cdot (\rho \mathbf{u}\mathbf{u} + P\mathbf{I} - \mathbf{b}\mathbf{b}) = \nabla \cdot \boldsymbol{\tau}, \tag{14}$$

$$\frac{\partial \mathbf{b}}{\partial t} + \nabla \cdot (\mathbf{u}\mathbf{b} - \mathbf{b}\mathbf{u}) + \nabla \times \left[\frac{1}{\sigma}(\nabla \times \mathbf{b}) \right] = 0, \tag{15}$$

$$\frac{\partial E}{\partial t} + \nabla \cdot [(E+P)\mathbf{u} - (\mathbf{b}\cdot\mathbf{u})\mathbf{b}] = +\nabla \cdot \left(\mathbf{u}\cdot\boldsymbol{\tau} + \mathbf{Q} + \left(\frac{\mathbf{b}}{\sigma}\cdot\nabla\mathbf{b} - \nabla\mathbf{b}\cdot\frac{\mathbf{b}}{\sigma} \right) \right), \tag{16}$$

where $E = \rho Z = \rho(e + \mathbf{u}^2/2) + \mathbf{b}^2/2$ is the total energy, $P = p + \|\mathbf{b}\|^2/2$ the total pressure, $Q = \lambda \nabla T$ is the heat flux with λ the thermal conductivity.

These equations can be non-dimensionalized by the quantities: length scale L, ρ_{ref}, u_{ref}, B_{ref}, $\mu_{m_{\mathrm{ref}}}$, T_{ref}, and σ_{ref}. The non-dimensional quantities appearing in the equations are

$$t^\star = tL/U_{\mathrm{ref}}, \quad \rho^\star = \rho/\rho_{\mathrm{ref}}, \quad T^\star = T/T_{\mathrm{ref}},$$
$$U^\star = U/U_{\mathrm{ref}}, \quad \mathbf{B}^\star = \mathbf{B}/\mathbf{B}_{\mathrm{ref}}, \quad p^\star = p/\rho_{\mathrm{ref}}U_{\mathrm{ref}}^2,$$
$$\mu^\star = \mu/\mu_{\mathrm{ref}}, \quad \mu_{\mathrm{m}}^\star = \mu_{\mathrm{m}}/\mu_{m_{\mathrm{ref}}}, \quad \sigma^\star = \sigma/\sigma_{\mathrm{ref}}.$$

In the following the asterisk superscript will be dropped for notational convenience. Therefore all the quantities will be assumed to be adimensionalized. The non-dimensional form of Eqs. (13)–(16) is

$$\frac{\partial \rho}{\partial t} + \nabla \cdot (\rho \mathbf{u}) = 0, \tag{17}$$

$$\frac{\partial \rho \mathbf{u}}{\partial t} + \nabla \cdot (\rho \mathbf{u}\mathbf{u} + P\mathbf{I} - R_{\mathrm{b}}\mathbf{b}\mathbf{b}) = \frac{1}{Re}\nabla \cdot \boldsymbol{\tau}, \tag{18}$$

$$\frac{\partial \mathbf{b}}{\partial t} + \nabla \cdot (\mathbf{u}\mathbf{b} - \mathbf{b}\mathbf{u}) = -\frac{1}{Re_\sigma}\nabla \times \left[\frac{1}{\sigma}(\nabla \times \mathbf{b}) \right], \tag{19}$$

$$\frac{\partial E}{\partial t} + \nabla \cdot [(E+P)\mathbf{u} - R_{\mathrm{b}}(\mathbf{b}\cdot\mathbf{u})\mathbf{b}] = \nabla \cdot \mathbf{F}^{\mu}, \tag{20}$$

where

$$P = p + R_{\mathrm{b}}\left(\mathbf{b}^2/2 \right),$$
$$E = p/(\gamma-1) + \mathbf{u}^2/2 + R_{\mathrm{b}}(\mathbf{b}^2/2),$$
$$\mathbf{F}^{\mu} = \frac{1}{Re}\mathbf{u}\cdot\boldsymbol{\tau} + \frac{1}{(\gamma-1)PrM^2Re}\mathbf{Q} + \frac{R_{\mathrm{b}}}{Re_\sigma}\left(\frac{\mathbf{b}}{\sigma}\cdot\nabla\mathbf{b} - \nabla\mathbf{b}\cdot\frac{\mathbf{b}}{\sigma} \right),$$

with $Re = \rho_{\mathrm{ref}}U_{\mathrm{ref}}L/\mu_{\mathrm{ref}}$ is the Reynolds number, $Pr = \mu_{\mathrm{ref}}C_p/\lambda = 0.72$ is the Prandtl number, $M = U_{\mathrm{ref}}/\sqrt{\gamma r T_{\mathrm{ref}}}$ is the Mach number, $R_{\mathrm{b}} = B_{\mathrm{ref}}^2/\rho_{\mathrm{ref}}U_{\mathrm{ref}}^2\mu_{m_{\mathrm{ref}}}$ is the magnetic force number and $Re_\sigma = LU_{\mathrm{ref}}\mu_{m_{\mathrm{ref}}}\sigma_{\mathrm{ref}}$ is the magnetic Reynolds number.

3. Pseudo-wave scheme for 1D ideal MHD equations

The equations under pseudo-wave form are obtained by first writing an approximate Riemann solver as described by Powell et al. [11] for the 1D non-viscous part of the Eqs. (17)–(20). It is convenient to consider these equations under symmetrizable form, in terms of primitive variables

$$\mathbf{W} = (\rho, u, v, w, b_x, b_y, b_z, p)^{\mathrm{T}}$$

as a quasilinear system, written as

$$\frac{\partial \mathbf{W}}{\partial t} + (\mathbf{A_x}, \mathbf{A_y}, \mathbf{A_z}) \cdot \nabla \mathbf{W} = 0, \tag{21}$$

where $\mathbf{A_x}$, $\mathbf{A_y}$ and $\mathbf{A_z}$ are the jacobian matrices of the hyperbolic system in each space direction. The components of the jacobian matrices are given in [11], but are not explicitly required in the following.

Thereafter, for simplicity, the equations are derived for $\mathbf{n} = \mathbf{x}$. Therefore, the Riemann invariant relationships are obtained by writing the scaled left eigenvectors ℓ of the eigensystem matrix

$$\mathbf{A_n} = (\mathbf{A_x}, \mathbf{A_y}, \mathbf{A_z}) \cdot \mathbf{n},$$

where $\mathbf{n}$ is the direction of the space derivative. The eigensystem of the governing equations under quasi-conservative and symmetrizable form has eight eigenvalues corresponding to different waves, as discussed in [11]. The eigenvalues are

- $\lambda_{\mathrm{E}} = u$ corresponding to an entropy wave,
- $\lambda_{\mathrm{M}} = u$ corresponding to a magnetic field divergence wave,
- $\lambda_{\mathrm{A}^{\pm}} = u \pm c_{\mathrm{A}}^{x}$ corresponding to a pair of Alfvén waves with $c_{\mathrm{A}}^{x} = \frac{|b_x|}{\sqrt{\rho}}$,
- $\lambda_{\mathrm{F}^{\pm}} = u \pm c_{\mathrm{f}}^{x}$ corresponding to a pair of fast magnetoacoustic waves,
- $\lambda_{\mathrm{S}^{\pm}} = u \pm c_{\mathrm{s}}^{x}$ corresponding to a pair of slow magnetoacoustic waves,

with $c_{\mathrm{f,s}}^{x}$ the magnetoacoustic wave speed along $\mathbf{x}$ given by

$$(c_{\mathrm{f,s}}^{x})^2 = \frac{1}{2}\left(\frac{\gamma p + R_{\mathrm{b}}\mathbf{b}\cdot\mathbf{b}}{\rho} \pm \sqrt{\left(\frac{\gamma p + R_{\mathrm{b}}\mathbf{b}\cdot\mathbf{b}}{\rho}\right)^2 - 4\frac{\gamma p}{\rho}c_{\mathrm{A}}^{x\,2}}\right).$$

The second wave has a zero eigenvalue in the fully conservative case, but in the symmetrizable case, an eigenvalue equal to the normal component of the velocity. This wave describes the jump in the normal component of the magnetic field at discontinuities and leads to an equation stating that $\frac{\nabla\cdot\mathbf{b}}{\rho}$ is a passive scalar for the system. The danger of the not fully conservative formulation is that terms of order $\nabla\cdot\mathbf{b}$ are added, to what would be a divergence form (the one without the source term). However, in the case of flows without shock, as considered here, the added terms are negligible. Moreover, an other key property for wave propagation simulation is that this system under not fully conservative formulation is Galilean invariant.

The eigenvectors are unique except for a scaling factor. We use in this work, the choice given by Roe and Balsara [12] by using the coefficients:

$$(\alpha_{\mathrm{f}}^{x})^2 = \frac{a^2 - c_{\mathrm{s}}^{x2}}{c_{\mathrm{f}}^{x2} - c_{\mathrm{s}}^{x2}}, \quad (\alpha_{\mathrm{s}}^{x})^2 = \frac{c_{\mathrm{f}}^{x2} - a^2}{c_{\mathrm{f}}^{x2} - c_{\mathrm{s}}^{x2}},$$
$$\beta_y^{x} = \frac{b_y}{\sqrt{b_y^2 + b_z^2}}, \quad \beta_z^{x} = \frac{b_z}{\sqrt{b_y^2 + b_z^2}}.$$

Hence, the scaled left eigenvectors and corresponding eigenvalues are

- Entropy

$$\lambda_{\mathrm{E}} = u, \tag{22}$$
$$\ell_{\mathrm{E}} = \left(1, 0, 0, 0, 0, 0, 0, -\frac{1}{a^2}\right). \tag{23}$$

- Magnetic field divergence wave

$$\lambda_M = u, \tag{24}$$
$$\ell_M = (0, 0, 0, 0, 1, 0, 0, 0). \tag{25}$$

- Alfvén waves

$$\lambda_{\mathrm{A}} = u \pm R_{\mathrm{b}}^{1/2}\frac{b_x}{\sqrt{\rho}}, \tag{26}$$

$$\ell_{\mathrm{A}} = \left(0, 0, -\frac{\beta_z^x}{\sqrt{2}}, \frac{\beta_y^x}{\sqrt{2}}, 0, \pm\frac{\beta_z^x}{\sqrt{2\rho}}, \mp\frac{\beta_y^x}{\sqrt{2\rho}}, 0\right). \tag{27}$$

- Fast magnetoacoustic waves

$$\lambda_{F^\pm} = u \pm c_{\mathrm{f}}^x, \tag{28}$$

$$\ell_{F^\pm} = \left(0, \pm\frac{\alpha_{\mathrm{f}}^x c_{\mathrm{f}}}{2a^2}, \mp\frac{\alpha_{\mathrm{s}}^x c_{\mathrm{s}}^x}{2a^2}\beta_y^x \operatorname{sign} b_x, \mp\frac{\alpha_{\mathrm{s}}^x c_{\mathrm{s}}^x}{2a^2}\beta_z^x \operatorname{sign} b_x, 0, \frac{\alpha_{\mathrm{s}}^x \beta_y^x}{2a\sqrt{\rho}}, \frac{\alpha_{\mathrm{s}}^x \beta_z^x}{2a\sqrt{\rho}}, \frac{\alpha_{\mathrm{f}}^x}{2a^2\rho}\right). \tag{29}$$

- Slow magnetoacoustic waves

$$\lambda_{S^\pm} = u \pm c_{\mathrm{s}}^x, \tag{30}$$

$$\ell_{S^\pm} = \left(0, \pm\frac{\alpha_{\mathrm{s}}^x c_{\mathrm{s}}^x}{2a^2}, \pm\frac{\alpha_{\mathrm{f}}^x c_{\mathrm{f}}^x}{2a^2}\beta_y^x \operatorname{sign} b_x, \pm\frac{\alpha_{\mathrm{f}}^x c_{\mathrm{f}}^x}{2a^2}\beta_z^x \operatorname{sign} b_x, 0, -\frac{\alpha_{\mathrm{f}}^x \beta_y^x}{2a\sqrt{\rho}}, -\frac{\alpha_{\mathrm{f}}^x \beta_z^x}{2a\sqrt{\rho}}, +\frac{\alpha_{\mathrm{s}}^x}{2a^2\rho}\right). \tag{31}$$

Then, we obtain eight relationships satisfied by the solution of the Eq. (21) asserting that there exists eight quantities which are constant along characteristic paths, defined by $dx/dt = \lambda_X$, and corresponding to the eight ideal MHD propagating waves. These are obtained by writing $\mathrm{d}X = \ell_X \cdot \mathrm{d}W^{\mathrm{T}} = \ell_X \cdot (\mathrm{d}\rho, \mathrm{d}u, \mathrm{d}v, \mathrm{d}w, \mathrm{d}b_x, \mathrm{d}b_y, \mathrm{d}b_z, \mathrm{d}p)^{\mathrm{T}} = 0$ along each characteristic, with $X = E, M, A^\pm, F^\pm, S^\pm$, where the left hand sides of these equations are given by

- Entropy

$$\mathrm{d}E = \mathrm{d}\rho - \frac{\mathrm{d}p}{a^2}. \tag{32}$$

- Magnetic field divergence wave

$$\mathrm{d}M = R_{\mathrm{b}}^{1/2}\mathrm{d}b_x. \tag{33}$$

- Alfvén waves

$$\mathrm{d}A^\pm = -\frac{\beta_z^x}{\sqrt{2}}\mathrm{d}v + \frac{\beta_y^x}{\sqrt{2}}\mathrm{d}w \pm \frac{\beta_z^x}{\sqrt{2\rho}}\mathrm{d}b_y \mp \frac{\beta_y^x}{\sqrt{2\rho}}\mathrm{d}b_z. \tag{34}$$

- Fast magnetoacoustic waves

$$\mathrm{d}F^\pm = \pm\frac{\alpha_{\mathrm{f}}^x c_{\mathrm{f}}^x}{2a^2}\mathrm{d}u \mp \frac{\alpha_{\mathrm{s}}^x c_{\mathrm{s}}^x}{2a^2}\beta_y^x \operatorname{sign} b_x \mathrm{d}v \mp \frac{\alpha_{\mathrm{s}}^x c_{\mathrm{s}}^x}{2a^2}\beta_z^x \operatorname{sign} b_x \mathrm{d}w + R_{\mathrm{b}}^{1/2}\left(+\frac{\alpha_{\mathrm{s}}^x \beta_y^x}{2a\sqrt{\rho}}\mathrm{d}b_y + \frac{\alpha_{\mathrm{s}}^x \beta_z^x}{2a\sqrt{\rho}}\mathrm{d}b_z\right) + \frac{\alpha_{\mathrm{f}}^x}{2a^2\rho}\mathrm{d}p. \tag{35}$$

- Slow magnetoacoustic waves

$$\mathrm{d}S^\pm = \pm\frac{\alpha_{\mathrm{s}}^x c_{\mathrm{s}}^x}{2a^2}\mathrm{d}u \pm \frac{\alpha_{\mathrm{f}}^x c_{\mathrm{f}}^x}{2a^2}\beta_y^x \operatorname{sign} b_x \mathrm{d}v \pm \frac{\alpha_{\mathrm{f}}^x c_{\mathrm{f}}^x}{2a^2}\beta_z^x \operatorname{sign} b_x \mathrm{d}w - R_{\mathrm{b}}^{1/2}\left(\frac{\alpha_{\mathrm{f}}^x \beta_y^x}{2a\sqrt{\rho}}\mathrm{d}b_y + \frac{\alpha_{\mathrm{f}}^x \beta_z^x}{2a\sqrt{\rho}}\mathrm{d}b_z\right) + \frac{\alpha_{\mathrm{s}}^x}{2a^2\rho}\mathrm{d}p. \tag{36}$$

These equations are straightforwardly obtained by multiplying the system

$$\frac{\partial \mathbf{W}}{\partial t} + \mathbf{A}_{\mathbf{n}} \cdot \nabla \mathbf{W} = 0,$$

on the left, successively, by the left eigenvectors ℓ_X, with $X = E, M, A^\pm, F^\pm, S^\pm$.

Therefore, for each mhd invariant $X = E, M, A^\pm, F^\pm, S^\pm$, the hyperbolic system gives the relations:

$$\frac{\mathrm{d}X}{\mathrm{d}t} = \frac{\partial X}{\partial t} + \lambda_X \cdot \frac{\partial X}{\partial x} = 0, \tag{37}$$

where λ_X is the corresponding eigenvalue.

By substituting the expression (32)–(36) into Eq. (37) and by using linear combinations of what is obtained, we isolate the time derivative of each primitive variable. The hyperbolic system under primitive variable form can then be written, with advective term $X_x = \lambda_X \cdot \frac{\partial X}{\partial x}$, as:

$$\frac{\partial p}{\partial t} = X^p, \quad \frac{\partial s}{\partial t} = X^s, \tag{38}$$

$$\frac{\partial u}{\partial t} = X^u, \quad \frac{\partial b_x}{\partial t} = X^{b_x}, \tag{39}$$

$$\frac{\partial v}{\partial t} = X^v, \quad \frac{\partial b_y}{\partial t} = X^{b_y}, \tag{40}$$

$$\frac{\partial w}{\partial t} = X^w, \quad \frac{\partial b_z}{\partial t} = X^{b_z}, \tag{41}$$

where

$$X^p = -\rho a^2[\alpha_f^x(F_x^+ + F_x^-) + \alpha_s^x(S_x^+ + S_x^-)],$$

$$X^u = \alpha_f^x c_f^x(F_x^+ - F_x^-) - \alpha_s^x c_s^x(S_x^+ - S_x^-),$$

$$X^v = +\frac{\beta_z^x}{\sqrt{2}}(A_x^+ + A_x^-) - \beta_y^x \operatorname{sign} b_x[\alpha_s^x c_s^x(F_x^+ - F_x^-) - \alpha_f^x c_f^x(S_x^+ - S_x^-)],$$

$$X^w = -\frac{\beta_y^x}{\sqrt{2}}(A_x^+ + A_x^-) - \beta_z^x \operatorname{sign} b_x[\alpha_s^x c_s^x(F_x^+ - F_x^-) - \alpha_f^x c_f^x(S_x^+ - S_x^-)],$$

$$X^{b_x} = -M_x/R_b^{1/2},$$

$$X^{b_y} = \frac{1}{R_b^{1/2}}\left[-\beta_z^x\sqrt{\frac{\rho}{2}}(A_x^+ - A_x^-) - \beta_y^x a\sqrt{\rho}\left[\alpha_s^x(F_x^+ + F_x^-) - \alpha_f^x(S_x^+ + S_x^-)\right]\right],$$

$$X^{b_z} = \frac{1}{R_b^{1/2}}\left[+\beta_y^x\sqrt{\frac{\rho}{2}}(A_x^+ - A_x^-) - \beta_z^x a\sqrt{\rho}\left[\alpha_s^x(F_x^+ + F_x^-) - \alpha_f^x(S_x^+ + S_x^-)\right]\right],$$

$$X^s = -E_x.$$

4. Extension to multidimensional non-ideal MHD

The Lorentz force acting on the gas particles produces an additional entropy alteration mechanism which is the Joule heating. This dissipative mechanism contributes to internal energy and entropy production. And therefore in the non-ideal MHD case, the three entropy sources are the following physical processes: thermal conduction, Joule heating and heating due to the viscosity.

The $(p, \mathbf{u}, \mathbf{b}, s)$ system can be written with additional viscous terms:

$$\frac{\partial p}{\partial t} + \mathbf{u}\cdot\nabla p = \gamma p \nabla\cdot\mathbf{u} + \frac{p}{C_v}\left(\frac{\partial s}{\partial t} + \mathbf{u}\cdot\nabla s\right), \tag{42}$$

$$\frac{\partial s}{\partial t} + \mathbf{u}\cdot\nabla s = \frac{S^\mu}{p}, \tag{43}$$

with

$$S^\mu = R\left(\frac{1}{(\gamma-1)PrM^2Re}\nabla\cdot\mathbf{Q} + \frac{R_b}{Re_\sigma}\frac{\mathbf{j}^2}{\sigma} + \frac{1}{Re}\boldsymbol{\tau}:\nabla\mathbf{u}\right).$$

Therefore, the two-dimensional viscous governing equations can be written as

$$\frac{\partial p}{\partial t} = X^p + Y^p + S^\mu/C_v, \tag{44}$$

$$\frac{\partial u}{\partial t} = X^u + Y^u + U^\mu/\rho, \tag{45}$$

$$\frac{\partial v}{\partial t} = X^v + Y^v + V^\mu/\rho, \tag{46}$$

$$\frac{\partial w}{\partial t} = X^w + Y^w + W^\mu/\rho, \tag{47}$$

$$\frac{\partial b_x}{\partial t} = X^{b_x} + Y^{b_x} + B_x^\mu, \tag{48}$$

$$\frac{\partial b_y}{\partial t} = X^{b_y} + Y^{b_y} + B_y^\mu, \tag{49}$$

$$\frac{\partial b_z}{\partial t} = X^{b_z} + Y^{b_z} + B_z^\mu, \tag{50}$$

$$\frac{\partial s}{\partial t} = X^s + Y^s + S^\mu/p, \tag{51}$$

where the $Y^{p,u,v,w,b_x,b_y,b_z,s}$ terms can be obtained by circular permutation of reference frame axes in relations (38)–(41), cf. Appendix A, and where the viscous terms are written as

$$U^{\mu} = \frac{1}{Re}\frac{\partial \tau_{1j}}{\partial x_j}, \qquad B_x^{\mu} = \frac{1}{Re_{\sigma}}\frac{\partial}{\partial x_j}\frac{1}{\sigma}\left(\frac{\partial b_1}{\partial x_j} - \frac{\partial b_j}{\partial x_1}\right),$$
$$V^{\mu} = \frac{1}{Re}\frac{\partial \tau_{2j}}{\partial x_j}, \qquad B_y^{\mu} = \frac{1}{Re_{\sigma}}\frac{\partial}{\partial x_j}\frac{1}{\sigma}\left(\frac{\partial b_2}{\partial x_j} - \frac{\partial b_j}{\partial x_2}\right),$$
$$W^{\mu} = \frac{1}{Re}\frac{\partial \tau_{3j}}{\partial x_j}, \qquad B_z^{\mu} = \frac{1}{Re_{\sigma}}\frac{\partial}{\partial x_j}\frac{1}{\sigma}\left(\frac{\partial b_3}{\partial x_j} - \frac{\partial b_j}{\partial x_3}\right).$$

5. Boundary conditions

We can distinguish two different types of numerical boundary conditions. The first case is when the numerical domain frontier correspond to the interface between two media. In a stationary frame of reference, the set of boundary conditions for the electromagnetic field requires that the normal components of magnetic flux density **B** and the tangential components of the electric fields are continuous across media interface. The difference between normal components of the electric field strength **E** is balanced by the surface charge density ρ_s. Finally, the discontinuity of the tangential components of the magnetic field density **B** is equal to the surface current density $\mathbf{j}_s$. The second case is when the boundary of the numerical domain gives rise to an open boundary condition, corresponding, for example, to an inflow or outflow physical setup. This boundary is then purely numerical, but generally produces unphysical spurious wave reflections due to the decrease of the numerical scheme order near the frontier.

With the pseudo-wave decomposition, the boundary conditions satisfying the non-ideal MHD equations can be easily imposed for a physical solid boundary between two media as well as for outlet or inlet conditions.

5.1. Non-reflecting boundary conditions

An interesting case is the non-reflecting boundary condition, which is imposed by avoiding on the box limit the contribution of the incoming waves obtained by checking the eigenvalue λ_X corresponding to different wave types $X = E_x, M_x, F_x^{\pm}, A_x^{\pm}, S_x^{\pm}$. For example at the left boundary of the computational box, where λ_X is positive, i.e. if the X-wave is incoming, X_x is fixed to zero.

5.2. Subsonic inflow boundary conditions

The subsonic inflow condition consists in prescribing the variation of five unknowns at the boundary nodes corresponding to five incoming waves. Different cases are possible, for example, the quantities $\partial s/\partial t$, $\partial u/\partial t$, $\partial v/\partial t$, $\partial w/\partial t$, $\partial b_x/\partial t$ can be prescribed to obtain the contribution of the incoming waves M_x, E_x, F_x^+, A_x^+, S_x^+ to the temporal variation on the boundary:

$$M_x = \frac{\partial b_x}{\partial t} - Y^{b_x} - B_x^{\mu},$$
$$E_x = \frac{\partial s}{\partial t} - Y^{s} - S^{\mu}/p,$$
$$F_x^+ = F_x^- + \frac{c_f^x \alpha_f^x}{a^2}\left(\frac{\partial u}{\partial t} - Y^u - U^{\mu}/\rho\right) + \frac{c_s^x \alpha_s^x}{a^2}\operatorname{sign} b_x(\beta_y^x X^v + \beta_z^x X^w),$$
$$A_x^+ = A_x^- - \sqrt{2}(\beta_y^x X^w - \beta_z^x X^v),$$
$$S_x^+ = S_x^- + \frac{c_s^x \alpha_s^x}{a^2}\left(\frac{\partial u}{\partial t} - Y^u - U^{\mu}/\rho\right) - \frac{c_f^x \alpha_f^x}{a^2}\operatorname{sign} b_x(\beta_y^x X^v + \beta_z^x X^w),$$

where the quantities X^u,X^v and X^w are given by the relations (45)–(47), and with

$$X^u = \frac{\partial u}{\partial t} - Y^u - U^{\mu}/\rho,$$
$$X^v = \frac{\partial v}{\partial t} - Y^v - V^{\mu}/\rho,$$
$$X^w = \frac{\partial w}{\partial t} - Y^w - W^{\mu}/\rho.$$

6. Numerical method

The new decomposition based on the p, u, b, s variables permits one to naturally use high-order upwind schemes to enforce numerical stability and minimize the numerical dissipation. The time-marching DRP schemes are developed by optimizing the finite difference approximations of the space and time derivatives in the wave number and frequency space [19]. These schemes have a good behavior for the radiation boundary conditions causing little acoustic reflections.

In this work all the inviscid fluxes appear in a quasilinear form and can be written under the generic form $(u\frac{\partial\phi}{\partial x})$ where u is a fluid velocity component and ϕ the advected quantity. High-order upwind Dispersion Relation Preserving schemes are used for all fluxes to improve both the stability and numerical accuracy for this wave propagation problem.

At the interior nodes the fourth-order accurate upwind biased DRP scheme [20] is written as follows:

$$\left(u\frac{\partial\phi}{\partial x}\right) = u_i\frac{1}{\Delta x}\sum_{k=-4,2} a_k\phi_{i+k}, \tag{52}$$

with

$$a_{-4} = 0.0161404967151,\ \ a_{-3} = -0.122821279020,\ \ a_{-2} = 0.455332277706,$$
$$a_{-1} = -1.2492595882615,\ \ a_0 = 0.5018904380193,\ \ a_1 = 0.4399321927296,$$
$$a_2 = -0.04121453788895$$

when the convective velocity u is positive. This DRP scheme has to be modified near the computational domain boundaries as follows:

- At $i = 2$, the first-order upwind scheme is used

$$\left(u\frac{\partial\phi}{\partial x}\right) = u_i\frac{1}{\Delta x}\sum_{k=-1,0} a_k\phi_{i+k}, \tag{53}$$

with

$$a_{-1} = -1,\ \ a_0 = 1.$$

- At $i = 3$, the third-order upwind scheme is used

$$\left(u\frac{\partial\phi}{\partial x}\right) = u_i\frac{1}{\Delta x}\sum_{k=-2,1} a_k\phi_{i+k}, \tag{54}$$

with

$$a_{-2} = 1/6,\ \ a_{-1} = -1,\ \ a_0 = 1/2,\ \ a_1 = 1/3.$$

- At $i = 4$, the fifth-order upwind scheme is used

$$\left(u\frac{\partial\phi}{\partial x}\right) = u_i\frac{1}{\Delta x}\sum_{k=-3,2} a_k\phi_{i+k}, \tag{55}$$

with

$$a_{-3} = -1/30,\ \ a_{-2} = 1/4,\ \ a_{-1} = -1,\ \ a_0 = 1/3,\ \ a_1 = 1/2,\ \ a_2 = -1/20.$$

- At $i = Nx - 1$, the third-order upwind-biased DRP scheme proposed in [20] is used

$$\left(u\frac{\partial\phi}{\partial x}\right) = u_i\frac{1}{\Delta x}\sum_{k=-5,1} a_k\phi_{i+k}, \tag{56}$$

with

$$a_{-5} = -0.0306489732244242,\ \ a_{-4} = 0.202225858313369,\ \ a_{-3} = -0.634728026533812,$$
$$a_{-2} = 1.29629965415671,\ \ a_{-1} = -2.14305478803459,\ \ a_0 = 1.10888726751399,$$
$$a_1 = 0.201019007808754.$$

- At $i = Nxd$, the sixth order upwind scheme is used

$$\left(u\frac{\partial\phi}{\partial x}\right) = u_i\frac{1}{\Delta x}\sum_{k=-6,0} a_k\phi_{i+k}, \tag{57}$$

with

$$a_{-6} = 1/60,\ \ a_{-5} = -6/5,\ \ a_{-4} = 15/4,\ \ a_{-3} = 20/3,\ \ a_{-2} = 15/2,\ \ a_{-1} = -6,\ \ a_0 = 49/20.$$

The third order TVD Runge–Kutta scheme, proposed by Shu and Osher [18], is used for time discretization

$$u^{n,1} = u^n + \Delta t\left(\frac{\partial u^n}{\partial t}\right),$$
$$u^{n,2} = \frac{1}{4}\left(3u^n + u^{n,1} + \Delta t\left(\frac{\partial u^{n,1}}{\partial t}\right)\right),$$
$$u^{n+1} = \frac{1}{3}\left(u^n + 2u^{n,2} + 2\Delta t\left(\frac{\partial u^{n,2}}{\partial t}\right)\right).$$

This TVD temporal scheme is optimal in the sense of CFL coefficient as proved in [4] and is suitable for solving hyperbolic conservations laws with stable spatial discretization. The time step Δt is restricted as usual by a CFL condition, with

$$\Delta t = \mathrm{CFL} \cdot \min_{\Omega} \frac{\Delta x}{|u| + c_f},$$

where Ω is the computational domain.

7. Numerical validation

Three different physical cases, corresponding to different initial conditions, are considered: an Alfvén wave, 1D and 2D magnetosonic wave propagation and the MHD equivalent of the 1D Rayleigh problem for viscous assessment. The flow regime is characterized by two dimensional numbers, the sonic M and the alfvénic M_A Mach numbers. The background pressure p_0 is given by the Mach number and the background magnetic field b_0 by the Alfvénic Mach number.

7.1. Initial conditions

The background physical state in term of non-dimensional quantities pressure p, fluid velocity $\mathbf{u}$, magnetic field $\mathbf{b}$ and entropy s is given by

$$\rho_0 = 1,$$
$$p_0 = \frac{\rho_0}{\gamma M^2},$$
$$u_0 = 1,$$
$$b_0 = 1,$$
$$s_0 = C_v \ln(p^\gamma/\rho),$$

with $C_v = 1/M^2\gamma(\gamma - 1)$. Therefore, we will consider fluctuation propagations around these background states. Then the sonic velocity field is $c^2 = \gamma p/\rho$, the Alfvén wave velocity along x-axis is $c_A = b_x\sqrt{R_b/\rho}$.

7.2. Alfvén wave propagation

The Alfvén wave travels through the computational box of length $L = 15$ with the non-dimensional wave velocity $c_A = 1$. The computational box is periodic in both directions, the number of grid points is $Nx \times Ny = 51 \times 11$. The x components of the magnetic field and of the velocity field are

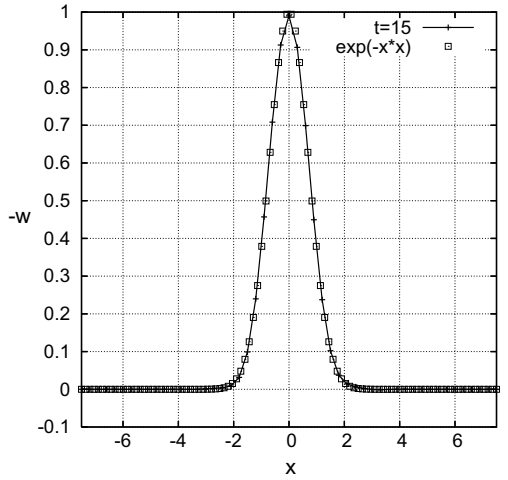

Fig. 1. Transverse velocity fluctuation $-w(x,t)$ for $c_A = 1$ and $u = u_0 = 1$: comparison between the computed solution at $t = 15$ and the initial condition.

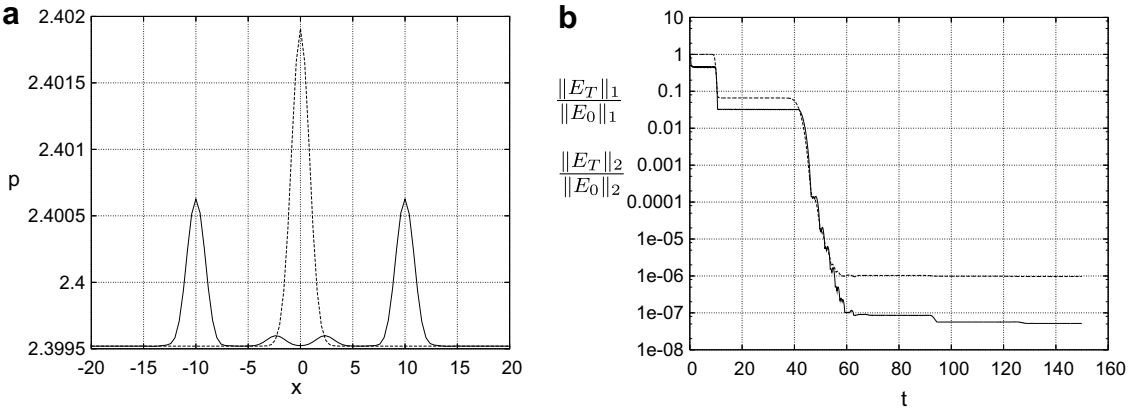

Fig. 2. (a) Snapshot of the pressure field at $t = 0$ (– –) and at $t = 4.83$ (—), (b) time evolution of $\frac{\|E_T\|_1}{\|E_0\|_1}$ (—) and $\frac{\|E_T\|_2}{\|E_0\|_2}$ (– –).

$$b_x = 1, \quad u = 0,$$

where these quantities are non-dimensional. Under these conditions, the solution to the governing equations is $b_z\sqrt{R_b/\mu_m\rho}(x,t) = -w(x,t) = f(x - c_A t)$, where $c_A = b_x\sqrt{R_b/\mu_m\rho}$ is the Alfvén velocity. In that case, μ_m, $R_b = 1/\sqrt{M_A}$ and ρ are set to unity. The Mach number is set to the low value $M = 10^{-2}$ to simulate a quasi-incompressible flow. At $t = 0$, the initial transverse magnetic field perturbation is $b_z\sqrt{(R_b/\mu_m\rho)} = e^{-x^2}$. The time step used for the simulation is fixed to $\Delta t = 5 \times 10^{-3}$ to provide time-step-independent results.

The Alfvén wave propagation is simulated until $t = 15$, that is the time, when the soliton wave form has traveled once through the computational box. The computed transverse component of the magnetic field at $t = 15$ is perfectly superposed to the initial wave at $t = 0$ as shown in Fig. 1. Therefore, the method has small dispersion and dissipation properties. Explicit and compact schemes have been benchmarked on the same setup in [3]. Our method gives result quality similar to high order (4th-order and 6th-order) spatially implicit schemes considered in conjunction with up to 10th-order filters, as introduced in [3].

7.3. Magnetosonic wave propagations

7.3.1. 1D pressure pulse: $M = 0.5$ and $M_A = 2$

The initial condition is a pulse of pressure given by

$$p(x,y,t=0) = p_0(1 + \varepsilon e^{\alpha x^2}), \tag{58}$$

$$\rho(x,y,t=0) = \rho_0(1 + M^2 p_0 \varepsilon e^{\alpha x^2}), \tag{59}$$

where R is the initial perturbation radius and $\alpha = -\ln(2)/R^2$. To validate the one dimensional case, we will use $u_0 = 0$ to easily compare the velocity wave to the theoretical speed without loss of generality. The b_x component is given by the Alfvénic Mach number. A non-zero value $b_z = 1$ is taken to allow simultaneously both slow and fast magnetoacoustic 1D wave propagation.

The simulations are performed for different sonic M and Alfvénic M_A Mach numbers. The perturbation amplitude pressure is set to $\varepsilon = 10^{-3}$ times the background reference pressure. The mesh consists of 51×11 grid points. We set the Mach number to the value $M = 0.01$, the magnetic permeability $\mu_m = 1$, the $CFL = 0.5$, the Reynolds number is $Re = \infty$ and the magnetic Reynolds number $Re_\sigma = \infty$.

Fig. 2(a) shows the pressure variation due to fast and slow magnetoacoustic waves traveling toward left and right with $c_s = 0.5$ and $c_f = 2$. The boundary conditions correspond to non-reflecting boundaries imposed by fixing the incoming waves to zero on the computing box boundary. The capacity to evacuate the energy fluctuations is shown in the Fig. 2(b). The ratio $\frac{\|E_T\|_2}{\|E_0\|_2}$ of energy fluctuations at the final time $t = 150$ to energy fluctuations at the initial time is around 10^{-6} (10^{-7} with $\|\cdot\|_1$ norm) and is slightly dependent on the physical setup considered, essentially in terms of sonic and Alfvénic Mach numbers. We observe in this time evolution the two decreases due to the outgoing of first the fast magnetosonic (at $t = 10$) and then the slow magnetosonic (at $t = 40$) waves, respectively.

7.3.2. 2D pressure pulse: $M = 0.9$ and $M_A = 2$

The initial condition is a pulse of pressure with a non-zero advection velocity given by

$$p(x,y,t=0) = p_0(1 + \varepsilon e^{\alpha r^2} t)$$

$$u(x,y,t=0) = u_0/\sqrt{2}, v(x,y,t=0) = u_0/\sqrt{2}, w(x,y,t=0) = 0$$

$$b_x(x,y,t=0) = b_0/\sqrt{2}, b_y(x,y,t=0) = b_0/\sqrt{2}$$
$$b_z(x,y,t=0) = 0$$
$$\rho(x,y,t=0) = \rho_0(1 + M^2 p_0 \varepsilon e^{\alpha r^2}),$$

where $r^2 = x^2 + y^2$ and $\alpha = -\ln(2)/R^2$. As in the 1D case, the pressure perturbation amplitude is set to $\varepsilon = 10^{-3}$ times the background reference pressure, the magnetic permeability to $\mu_m = 1$, the Reynolds number to $Re = \infty$ and the magnetic Reynolds number to $Re_\sigma = \infty$. The mesh consists of 201×201 grid points.

The initial pressure distribution is set to give rise to slow and fast magnetosonic waves. With $M = 0.9$ and $M_A = 2$, the slow and fast magnetosonic wave velocities are $c_s = 0.5$ and $c_f = 1.11$, respectively. Therefore in the direction of the magnetic field, both the right and left slow magnetosonic waves are advected in the direction of the magnetic field at speed $u_0 \pm c_s$ and $u_0 \pm c_f$ for the fast magnetosonic waves. Fig. 3 shows the time evolution of the pressure field. The wave propagation is anisotropic depending of the magnetic field direction. The wave expulsion is efficient with the imposed non-reflecting wave at the box boundaries for both slow and fast magnetosonic wave fronts.

7.4. Resistive diffusion assessment: The equivalent 1D Rayleigh problem

We consider the resistive diffusion of a magnetic field to validate the non-ideal components of the code for finitely conducting media. This problem is equivalent to the Rayleigh problem in fluid dynamics in which a sudden step velocity is imposed to the wall adjoining a viscous fluid. For the magnetic equivalent, a current sheet $j_z(y = -5, t \geqslant 0) = j_0$ is suddenly imposed at the boundary domain in a semi-infinite region. In the conducting fluid, outside the conductor, a uniform magnetic field $b_x(0, t > 0) = b_0$ which is parallel to the conductor surface, is induced. A no-slip condition $\mathbf{u}(0, t > 0) = 0$ is imposed at the boundary $(-5 \leqslant y \leqslant +5)$ together with the specified value of the magnetic field $b_x(0, t > 0) = b_0$ and $b_y(0, t > 0) = b_z(0, t > 0) = 0$. The theoretical solution can be written in terms of the error function as

$$b_x(y,t) = 2 - \frac{2}{\sqrt{\pi}} \int_{-\infty}^{\frac{y}{2\sqrt{t/Re_\sigma}}} e^{-\xi^2} d\xi.$$

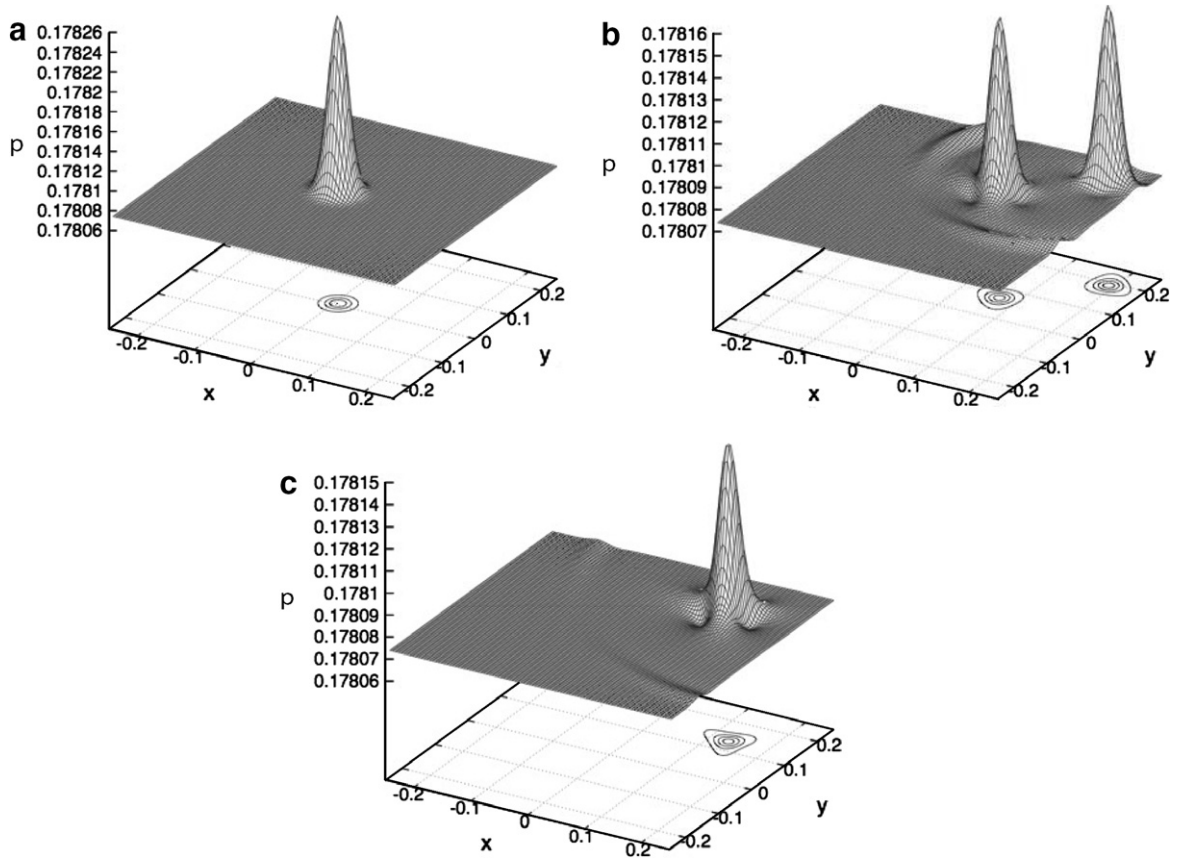

Fig. 3. Time evolution of the pressure field: (a) $t = 0$, (b) $t = 0.18$, (c) $t = 0.36$.

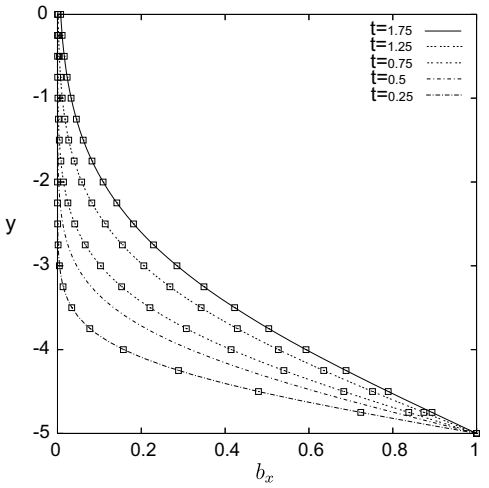

Fig. 4. Magnetic field diffusion at the boundary, theory (□), $t = 0.25$ (– · –), $t = 0.75$ (- · -), $t = 1.25$ (· · ·), $t = 1.75$ (· · · · · ·).

The Reynolds number is set to $Re = \infty$, the grid point number to $Ny = 100$ in the space range $-5 < y < +5$, the time step is fixed to $\Delta t = 10^{-3}$ to obtain time-step-independent results. The computed solution is plotted in Fig. 4 at several time instants for $Re_\sigma = 1$. The temporal evolution of the magnetic field is due to magnetic field diffusion into the conducting fluid. Fig. 4 shows that the results of the MHD calculations are indistinguishable from the theoretical solution.

8. Conclusions

A high order pseudo-wave numerical method has been developed to solve the governing equations of non-ideal MHD. The new formulation of the MHD equations exhibits the contribution of each different wave-type to the overall dynamics. A high-order DRP scheme is used for the spatial discretization and third order TVD Runge kutta for temporal advance. This method maintains a good stability and allows a boundary treatment consistent with the interior scheme. The present method can easily be extended to the three-dimensional case and/or multiblock simulations and so easily adapted to parallel intensive computational framework.

In the future, this code will be used to investigate the feasibility of electromagnetic laminar and turbulent flow control for which the physics of the boundary layer has to be very well captured. Moreover, this code could be very useful to better understand the magneto-aeroacoustic mechanisms in the MHD paradigm. Indeed, the good capacity of the method to treat the acoustic propagations and the corresponding boundary conditions, makes it a powerful tool to explore the different types of magnetoaeroacoustic sinks and sources as well as the related wave interaction mechanisms in a compressible conducting fluid.

Appendix A

The terms appearing in Eqs. (44)–(51) are given by the relations:

$$
\begin{aligned}
Y^p &= -\rho a^2[\alpha_{\mathrm{f}}^y(F_y^+ + F_y^-) + \alpha_{\mathrm{s}}^y(S_y^+ + S_y^-)],\\
Y^u &= \alpha_{\mathrm{f}}^y c_{\mathrm{f}}^y(F_y^+ - F_y^-) - \alpha_{\mathrm{s}}^y c_{\mathrm{s}}^y(S_y^+ - S_y^-),\\
Y^v &= +\frac{\beta_x^y}{\sqrt{2}}(A_y^+ + A_y^-) - \beta_z^y \operatorname{sign} b_z[\alpha_{\mathrm{s}}^y c_{\mathrm{s}}^y(F_y^+ - F_y^-) - \alpha_{\mathrm{f}}^y c_{\mathrm{f}}^y(S_y^+ - S_y^-)],\\
Y^w &= -\frac{\beta_z^y}{\sqrt{2}}(A_y^+ + A_y^-) - \beta_x^y \operatorname{sign} b_y[\alpha_{\mathrm{s}}^y c_{\mathrm{s}}^y(F_x^+ - F_x^-) - \alpha_{\mathrm{f}}^y c_{\mathrm{f}}^y(S_x^+ - S_x^-)],\\
Y^{b_x} &= -M_y/R_{\mathrm{b}}^{1/2},\\
Y^{b_y} &= \frac{1}{R_{\mathrm{b}}^{1/2}}\left[-\beta_x^y\sqrt{\frac{\rho}{2}}(A_x^+ - A_x^-) - \beta_z^y a\sqrt{\rho}\left[\alpha_{\mathrm{s}}^y\left(F_y^+ + F_y^-\right) - \alpha_{\mathrm{f}}^y\left(S_y^+ + S_y^-\right)\right]\right],\\
Y^{b_z} &= \frac{1}{R_{\mathrm{b}}^{1/2}}\left[+\beta_z^y\sqrt{\frac{\rho}{2}}(A_y^+ - A_y^-) - \beta_x^y a\sqrt{\rho}[\alpha_{\mathrm{s}}^y(F_y^+ + F_y^-) - \alpha_{\mathrm{f}}^y(S_y^+ + S_y^-)]\right],\\
Y^s &= -E_y,
\end{aligned}
$$

where

$$\alpha_s^y = \frac{c_f^{y2} - a^2}{c_f^{y2} - c_s^{y2}}, \qquad \alpha_f^y = \frac{a^2 - c_s^{y2}}{c_f^{y2} - c_s^{y2}},$$
$$\beta_x^y = \frac{b_x}{\sqrt{b_x^2 + b_z^2}}, \qquad \beta_z^y = \frac{b_z}{\sqrt{b_x^2 + b_z^2}}.$$

References

[1] A. Collis, Kaveh Ghayour, Matthias Heinkenschloss, Optimal transpiration boundary control for aeroacoustics, AIAA J. 41 (7) (2003) 1257–1270.
[2] M. Brio, C.C. Wu, An upwind differencing scheme for the equations of ideal magnetohydrodynamics, J. Comput. Phys. 75 (1988) 400–422.
[3] Datta V. Gaitonde, Higher-order solution procedure for three-dimensional nonideal magnetogasdynamics, AIAA J. 39 (11) (2001) 2111–2120.
[4] S. Gottlieb, Chi-Wang Shu, Total variation diminishing Runge–Kutta schemes, Math. Comput. 67 (1998) 73–85.
[5] R.S. Hirsch, Higher order accurate difference solutions of fluid mechanics problems by compact differencing technique, J. Comput. Phys. 19 (1) (1975) 90–109.
[6] O.S. Jones, U. Shumlak, D.S. Eberhardt, An implicit scheme for nonideal magnetohydrodynamics, J. Comput. Phys. 130 (1) (1997) 231–242.
[7] R. Lechner, J. Sesterhenn, R. Friedrich, Turbulent supersonic channel flow, J. Turbul. 2 (2001).
[8] S. Lele, Compact finite difference schemes with spectral-like resolution, J. Comput. Phys. 103 (1992) 16–42.
[9] S.Y. Lu, P. Sagaut, Pseudo-characteristic formulation and dynamic boundary conditions for computational aeroacoustics, Int. J. Numer. Meth. Fluids. 53 (2007) 201–227.
[10] R.W. MacCormack, Upwind conservation form method for the ideal magnetohydrodynamics equations, AIAA paper, 99-3609, 1999.
[11] K.G. Powell, P.L. Roe, T.J. Linde, T.I. Gombosi, D.L. De Zeeuw, A solution-adaptative upwind scheme for ideal magnetohydrodynamics, J. Comput. Phys. 154 (1999) 284–309.
[12] P.L. Roe, D.S. Balsara, Notes on the eigensystem of magnetohydrodynamics, SIAM J. Appl. Math. 56 (1) (1996) 57–67.
[13] J. Sesterhenn, A characteristic-type formulation of the Navier–Stokes equations for high order upwind schemes, Comput. Fluids (2001) 37–67.
[14] J.S. Shang, Recent research in magneto-aerodynamics, Progr. Aerospace Sci. 37 (2001) 1–20.
[15] J.S. Shang, Shared knowledge in computational fluid dynamics, electrodynamics and magneto-aerodynamics, Progr. Aerospace Sci. 38 (2002) 449–467.
[16] J.S. Shang, Three decades of accomplishments in computational fluid dynamics, Progr. Aerospace Sci. 40 (2004) 173–197.
[17] J.A. Shercliff, A textbook of magnetohydrodynamics, Pergamon, 1965.
[18] C. Shu, S. Osher, Efficient implementation of essentially non-oscillatory shock capturing schemes ii, J. Comput. Phys. 83 (1989) 32–78.
[19] C.K.W. Tam, J.C. Webb, Dispersion-relation-preservation difference schemes for computational acoustics, J. Comput. Phys. 107 (1993) 262–281.
[20] M. Zhuang, R. Chen, Applications of higher-order optimized upwind schemes for computational aeroacoustics, AIAA J. 40 (3) (2002) 443–449.